Detection and Analysis of Strong Ionospheric Scintillation in Equatorial Region

ZHU Xuefen, LIN Mengying, LU Zhengpeng, CHEN Xiyuan

(*Key Laboratory of Micro-Inertial Instrument and Advanced Navigation Technology of Ministry of Education*, *School of Instrument Science and Engineering*, *Southeast University*, *Nanjing* 210096, *China*)

Abstract: To detect the occurrence of ionospheric scintillation in the equatorial region, a coherent/non-coherent integration method is adopted on the accumulation of intermediate frequency (IF) signal and local code, in the process of signal acquisition based on software receiver. The processes of polynomial fitting and sixth-order Butterworth filtering are introduced to detrend the tracking results. Combining with ionospheric scintillation detection algorithm and preset thresholds, signal acquisition and tracking, scintillation detection, positioning solution are realized under the influence of strong ionospheric scintillation. Under the condition that the preset threshold of amplitude and carrier phase scintillation indices are set to 0.5 and 0.15, and the percentage of scintillation occurrence is 50%, respectively, PRN 12 and 31 affected by strong amplitude scintillation are detected effectively. Results show that the positioning errors in the horizontal direction are below 5m approximately. The software receiver holds performances of accurate acquisition, tracking and positioning on the strong ionospheric scintillation conditions, which can provide important basis and helpful guidance for relevant research on ionospheric scintillation, space weather and receiver design with high performance.

Keywords: Ionospheric Scintillation, Acquisition and Tracking; Positioning Error, Coherent/Non-coherent Integration, Detrending

1 Introduction

With the development and application of GPS and navigation technology, it is increasingly important to improve the security and reliability of satellite navigation systems. The observation and study of ionospheric scintillation, as a medium for signal propagation, which can produce a negative impact on the quality of the received global navigation satellite systems (GNSS) signal [1], has become one of the important contents and hotspots in space weather. In the ionosphere which is about 60 ~ 1000 kilometers from the ground, the atmosphere interacts with high-energy particles from the sun, making atmospheric molecules and atoms charged particles with uneven density distribution, and the ionospheric scintillation is a phenomenon that the amplitude and phase of signals fluctuate randomly when signals propagate through the plasma irregularly [2-3]. There are many reasons for this phenomenon, including magnetic storms, solar activity, local electric field, electrical conductivity, etc. It is also closely related to the geographical area, season, local time, geomagnetic activity [4], etc.

Ionospheric scintillation occurs mainly in the equatorial and polar regions [5]. The scintillations in equatorial region are mainly amplitude scintillation and in the polar region are mainly phase scintillation.

The frequency and intensity of ionospheric scintillation will increase in solar maximum year. Strong ionospheric scintillation will decrease signal quality and even cause signal tracking failure and make the receiver fail in navigation in serious cases [6-8]. Especially in the low latitudes during the solar maximum year, frequent and strong ionospheric scintillations lead to significant attenuation in intensity and carrier-to-noise ratio of signal [9-10]. Due to the suddenness of ionospheric scintillation, frequent and severe ionospheric scintillation makes detection and satellite signal acquisition and tracking more difficult, especially in the equatorial regions.

In this paper, the software receiver is used to detect and analyze the strong ionospheric scintillation in the equatorial regions. The results of analysis will provide powerful guidance for designing high-performance tracking algorithms and improving the sensitivity and robustness of satellite receivers. The South China Sea is a low-latitude and equatorial region in China. It is of great significance to design efficient ionospheric scintillation detection and high-performance receiver algorithms for the practical application of the Beidou navigation system and the territorial security of the South China Sea.

2 Ionospheric Scintillation Indices

Frequent strong ionospheric scintillations can easily affect the acquisition and tracking of satellite signals, and even lead to positioning and navigation failures in low-latitude areas in solar maximum year. In order to realize the accurate detection and acquisition of strong ionospheric scintillations in the equatorial regions, the coherent/non-coherent integration algorithm [11] is designed to improve the signal-to-noise ratio of the signal.

Considering the influence of noise signal, the satellite signal is processed by the receiver front-end and quantified by intermediate frequency sampling. Then the GNSS digital signal is correlated with the local code and the local carrier signal, and then two signals of the same phase component I and the quadrature component Q are obtained.

The coherent integration formula $\mathrm{I}_L = \sum_{n=0}^{L-1} \mathrm{I}(nT_s)$ and $\mathrm{Q}_L = \sum_{n=0}^{L-1} \mathrm{Q}(nT_s)$ are used to integrate the two signals respectively. After a series of mathematical operations, the formulas of two signals are as follows:

$$\mathrm{I}_L = \sqrt{2P_R} D_L R(\Delta\tau) \sin c(\pi \cdot \Delta f \cdot T_{coh}) \cos(\Delta\varphi) + \eta_I \quad (1)$$

$$\mathrm{Q}_L = \sqrt{2P_R} D_L R(\Delta\tau) \sin c(\pi \cdot \Delta f \cdot T_{coh}) \sin(\Delta\varphi) + \eta_Q \quad (2)$$

Where P_R is the average power of satellite signal, D_L is satellite spread spectrum code signal, $R(\bullet)$ is the correlation value between the received ranging code and the local code; η_I and η_Q are independent Gaussian white noise after accumulation, which obeys $N(0, L\sigma^2)$ in Gaussian distribution, σ^2 is the signal noise variance before coherent accumulation, $\Delta\tau = \tau - \bar{\tau}$ is the delay difference between the signal code and the local code, $\Delta f = f_d - \overline{f_d}$ is the frequency difference between received carrier signal and local carrier signal, $T_{coh} = L \cdot T_s$ is the product of sampling points L and the sampling period T_s, representing the coherent integration time, $\Delta\varphi$ is the difference of average phase after coherent integration.

Then, combined with the non-coherent integration method, the envelope of the accumulated value of the coherent integration is obtained. Firstly, the normalized noise variance of I and Q is obtained, and then noise components obey the N(0,1) distribution. The results of $\overline{\mathrm{I}_L}$ and $\overline{\mathrm{Q}_L}$ are non-coherently integrated M times, and the corresponding expression for this process is $\sum_{n=0}^{M} Z_L = \sum_{n=0}^{M} \sqrt{\overline{\mathrm{I}_L}^2 + \overline{\mathrm{Q}_L}^2}$. Finally, the acquisition of satellite signals is realized by acquisition decision.

The above coherent/non-coherent integration algorithm accurately captures the satellite signal and tracks it. In order to make the ionospheric scintillation indices accurately reflect the ionospheric scintillation, it is necessary to use detrending method to eliminate the fluctuation of tracking results caused by other factors. In the detrending process of ionospheric amplitude scintillation indices, we adopt the polynomial fitting method. Firstly, we calculate the standardized

signal strength:

$$WBP = \sum_{i=1}^{n} (I_i^2 + Q_i^2) \tag{3}$$

$$NBP = (\sum_{i=1}^{n} I_i)^2 + (\sum_{i=1}^{n} Q_i)^2 \tag{4}$$

Where the instantaneous code components I_i and Q_i of the same phase branch and the quadrature branch are measured to generate broadband power WBP and narrowband power NBP. If signal frequency of I_i and Q_i are 1000Hz, n is 60, and then the data length for power calculation is 60ms. Furthermore, we could calculate the signal strength:

$$S_{I,raw} = NBP - WBP \tag{5}$$

$$S_{I,norm} = \frac{S_{I,raw}}{S_{I,trend}} \tag{6}$$

Where $S_{I,raw}$ is the original signal strength, and then $S_{I,raw}$ is fitted by fourth-order polynomial to obtain $S_{I,trend}$.

In addition, in order to eliminate the influence of environmental noise in the amplitude scintillation indices, we need to exclude the amplitude scintillation indices generated by noise:

$$S4_{N_0} = \sqrt{\frac{100}{\overline{S/N_0}}\left[1 + \frac{500}{19\overline{S/N_0}}\right]} \tag{7}$$

Where $\overline{S/N_0}$ is the average of signal-to-noise ratio.

In scintillation detection, $S4$ is the amplitude scintillation indices representing the degree of signal attenuation, which is estimated as:

$$S4 = \sqrt{\frac{E\left(S_{I,norm}^2\right) - E\left(S_{I,norm}\right)^2}{E\left(S_{I,norm}\right)^2} - S4_{N_0}^2} \tag{8}$$

Where $E(\bullet)$ represents the expected value over a period of time, and the amount of data, which is used to obtain the expected value, is determined by the frequency of signal strength sampling and the expected time. When the sampling frequency is 1000Hz, the amount of data in 10s is 10000.

To reflect the fluctuation of the carrier phase, we define the phase scintillation indices as the standard deviation of the detrended carrier phase:

$$\sigma_\phi = \sqrt{E\left(\phi_{trend}^2\right) - E\left(\phi_{trend}\right)^2} \tag{9}$$

Where ϕ_{trend} is the detrended result from the carrier phase ϕ:

$$\phi = \phi_{raw} + \Delta\phi \tag{10}$$

Where the original carrier phase ϕ_{raw} is the phase offset caused by the Doppler shift. $\Delta\phi$ is the correction of the carrier phase and is corrected by the carrier phase detector (PLL) in tracking part of satellite receiver. $\Delta\phi$ also represents the phase error.

In order to eliminate noise, we use the sixth-order Butterworth high-pass filter [12] with a cutoff frequency of 0.1 Hz to detrend the carrier phase ϕ and finally obtain ϕ_{trend}. The six-order filter is composed of 3 cascaded second-order filters to improve the stability of the filter.

Fig.1 shows the time-varying information of the carrier phase, which is collected from GPS satellite No. 25 in the equatorial regions of Brazil on November 27, 2013. The right side of the longitudinal axis represents the original carrier phase value, and the left side of the longitudinal axis represents the corresponding detrended result of carrier phase by the sixth-order Butterworth at the same period.

In the shadow region, we can clearly observe that the detrended carrier phase fluctuates over time, indicating that the signal is affected by ionospheric scintillation.

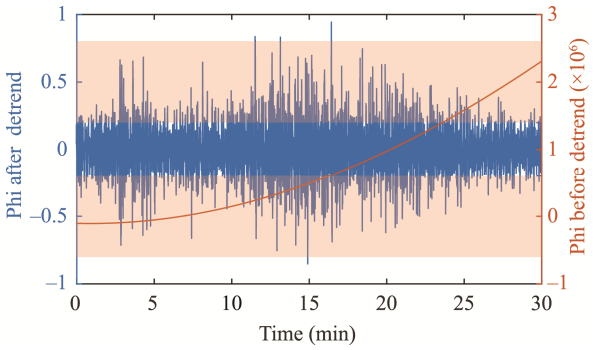

Fig.1 Comparison of Butterworth Filtering before and after

3 Detection System of Strong Ionospheric Scintillation

Ionospheric scintillation is a natural phenomenon

that it is difficult to predict the scintillation. In order to save data storage space, we combine the full-band receiving antenna with the commercial Septentrio receiver to monitor ionospheric scintillation. The acquisition system will be triggered to store data when a strong ionospheric scintillation is detected.

The software receiver receives the real-time satellite signal. After successfully tracking the signal, the software receiver collects the output and carrier phase data of I and Q channels, and then calculates the scintillation indices and judgment index of scintillation event in real time. The judgment index is compared with the set threshold.

If the trigger of the scintillation event is reached, the acquisition system will collect the multi-channel RF front-end data which is defined by the software and that data is the original IF data affected by ionospheric scintillation. The specific acquisition system is shown in Fig.2.

Because of the strong ionospheric scintillation in the equatorial regions, we adopt the coherent/non-coherent integration acquisition algorithm to improve the signal-to-noise ratio and achieve the purpose for accurate acquisition.

Compared with the serial search algorithm and the cyclic correlation algorithm [13], we adopt the coherent integration to improve the signal-to-noise ratio effectively, and then adopt the non-coherent integration to remove the limitation that the coherent integration time is easily affected by navigation data bit-flipping. Therefore, we can accurately capture satellite signals in a weak signal-to-noise ratio environment, which provides basic data for ionospheric scintillation detection.

For amplitude scintillation and phase scintillation, two different detrending methods, polynomial fitting and sixth-order Butterworth filtering, are taken to eliminate the influence of satellite motion, clock error and Doppler. By setting the scintillation threshold and recording the number of simultaneous occurrences of amplitude and phase scintillations, we successfully determine the occurrence of scintillations. The schematic diagram of ionospheric scintillation detection and analysis in software receiver is shown in Fig.3.

4 The Analysis of Ionospheric Scintillation Detection Data

Solar maximum year takes 11 years a cycle. Compared with other years, there is a frequent and strong ionospheric scintillation phenomenon in the Solar maximum year, and the latest year is 2013. Therefore, in order to test the feasibility of the designed algorithm under strong ionospheric scintillation mentioned in this paper, the data was collected by the data acquisition system deployed in the equatorial regions of Brazil on November 27, 2013. The specific location is shown in Fig.4:

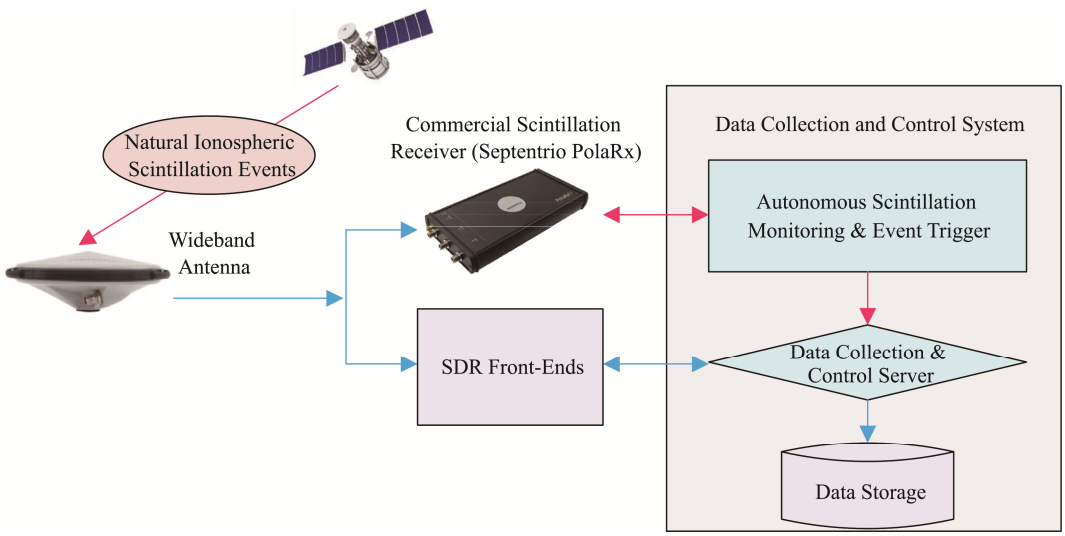

Fig.2 Data Collection System Driven by Ionospheric Scintillation

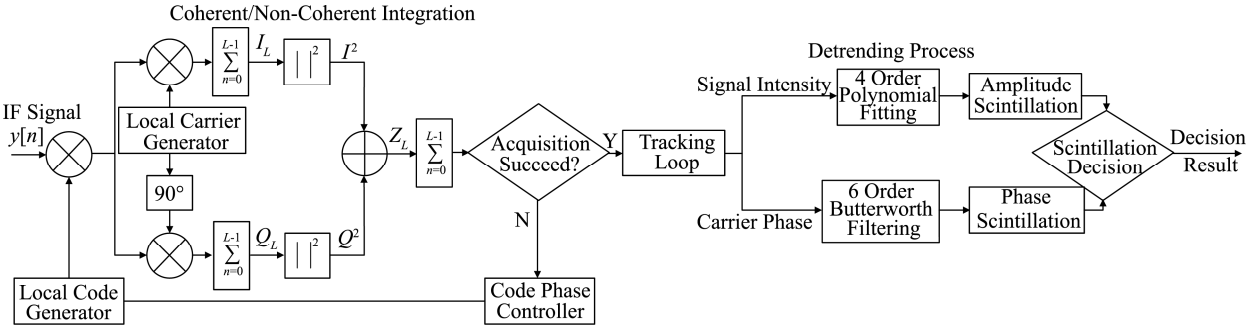

Fig.3 Principle of Ionospheric Scintillation Detection

Fig.4 Location of the Data Collection System on the Map

In MATLAB, we select the intermediate frequency signal of GPS L1 band recorded on November 27. We use the raw algorithm in GPS software receiver and acquisition algorithm improved by coherent/non-coherent integration to simulate the recorded data. The acquisition results corresponding to the two methods are shown in Fig.5.

Firstly, we set the acquisition threshold as 1.75. Satellite signals are seriously disturbed under the strong ionospheric scintillation, and the GPS software receiver with raw algorithm fail in capturing Satellite signal. As shown in Fig.5 (a).

The GPS receiver improved by the coherent/non-coherent integration algorithm captured 7 satellites, which were satellites 5, 12, 18, 21, 25, 29 and 31. As shown in Fig.5 (b).

In the case of successful acquisition, we track the signal. Fig.6 shows the tracking results of the instantaneous code phase and quadrature code phase of No. 25 satellite.

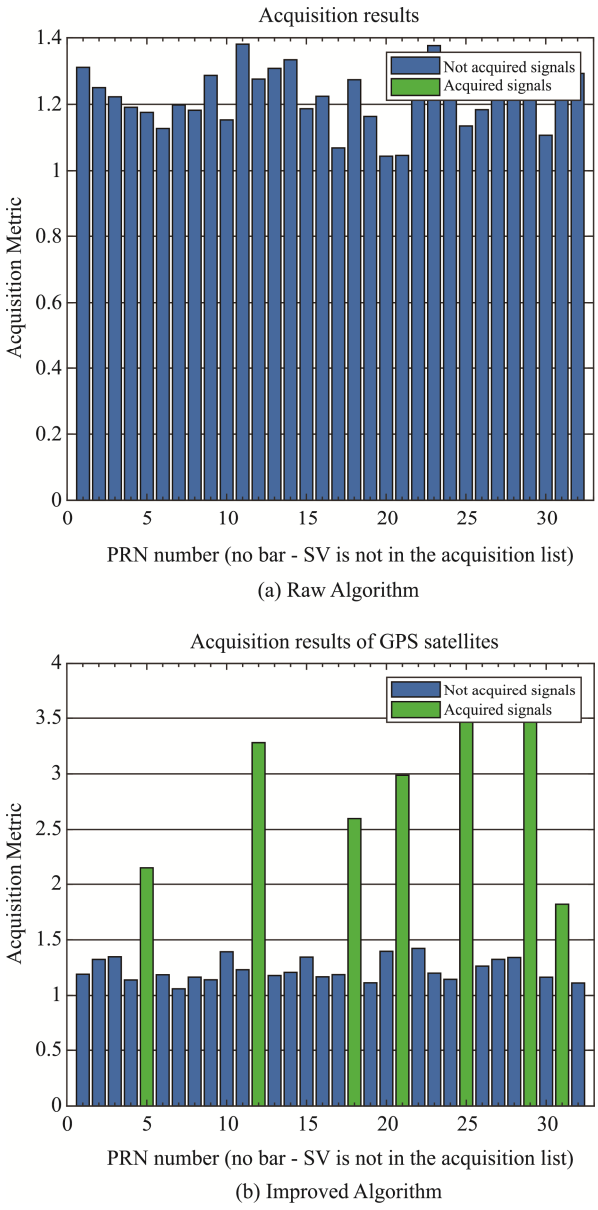

Fig.5 Acquisition under the Influence of Strong Ionospheric Scintillation

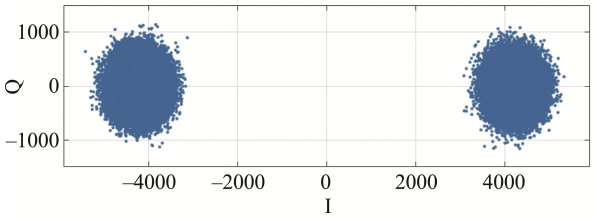

Fig.6 Tracking Results of GPS 25

Taking the tracking results of the captured satellite signal in GPS L1 band as an example, we detect the ionospheric scintillation within 1 hour, and discard the unstable data in the first 10 s, and the output frequency of scintillation indices is 1 Hz. The results are shown in Fig.7. Fig.7 (a) is the time-varying amplitude scintillation of GPS satellites 12, 18, 25 and 31, and Fig.7 (b) is the corresponding phase scintillation. When the amplitude scintillation indices S4 satisfies S4 < 0.2, it can be defined that there is no ionospheric scintillation; the amplitude scintillation indices satisfying 0.2< S4 < 0.5 is defined as weak scintillation; the amplitude scintillation indices satisfying S4 > 0.5 is defined as strong scintillation.

The red dotted line in Fig.7 (a) represents S4 = 0.5, and the moment that exceeds the red line indicates strong ionospheric scintillation occurs. Moreover, there is a small period of time when S4 is greater than 1, indicating that the scintillation reaches saturation, and that shows the signal is affected by strong ionospheric scintillation during this period.

In addition, since the detected signal comes from the Brazilian region near the equator, there should be relatively strong amplitude scintillation and relatively weak phase scintillation in signals. As is shown in Fig.7, strong amplitude scintillation is basically accompanied by phase scintillation, and the phase scintillation indices σ_ϕ satisfy σ_ϕ > 0.15 at some moments. The specific number and ratio of scintillation are shown in Table 1.

According to the ratio, amplitude scintillation mainly occurs in this region with lower intensity of phase scintillation. This result is consistent with the characteristics that there are mainly strong amplitude scintillations in equatorial and mainly phase scintillations in polar regions. The amplitude scintillation ratios of satellite No.12 and No.31 are 0.7339 and 0.6951, respectively. Therefore, in this period, the satellite signals are affected by strong ionospheric scintillation for more than 30 minutes. Meanwhile, the results show that satellites No. 18 and No. 25 are affected by strong ionospheric amplitude scintillation for nearly 30 minutes. Considering the factors such as the false acquisition of satellite signals and the enhancement of scintillation indices caused by other Interferences, we set the threshold of scintillation ratio to 50%. With this threshold, we successfully detected that satellites No. 12 and No. 31 were affected by strong ionospheric scintillation.

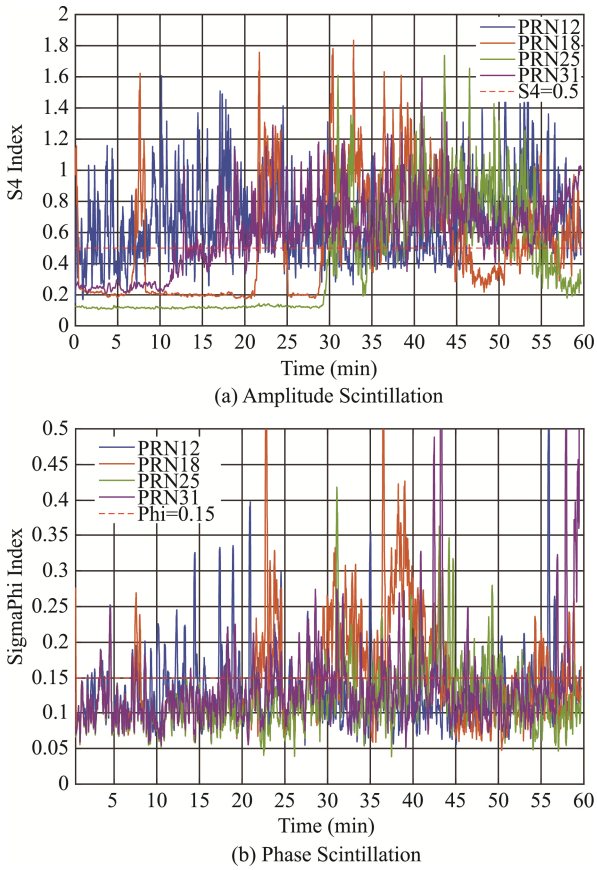

Fig.7 Ionospheric Scintillation Detection of GPS L1 Frequency

Table 1 Time and Proportion of Scintillation

PRN	Times of Scintillation		Ratio of Scintillation	
	S4>0.5	SigmaPhi>0.15	S4>0.5	SigmaPhi >0.15
12	2628	788	0.7339	0.2201
18	1598	1275	0.4462	0.3560
25	1324	762	0.3697	0.2128
31	2489	833	0.6951	0.2326

Taking actual acquisition point of satellite signal (Lat: –23°12′27.5772" Lng: –45°51′35.1414" Hgt: +693.4m) as reference, we test the positioning performance of the improved software receiver. The positioning error in the local cartesian coordinates coordinate system is shown in Fig. 8.

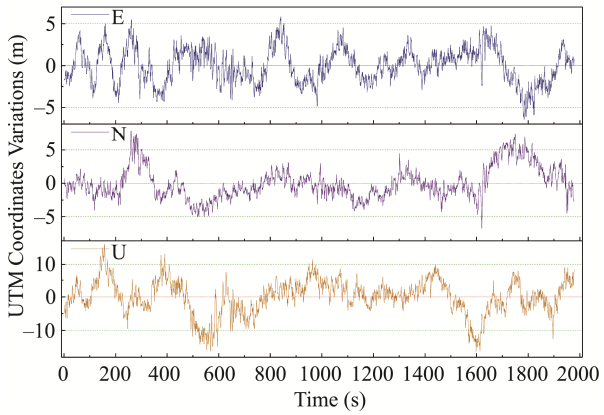

Fig.8 UTM Coordinates Variation

As shown in Fig.8, the horizontal direction error of the information calculated by the improved software receiver is controlled within 5 m, and height direction error is controlled within 10 m.

The satellite constellation after the data acquisition begins for 6 hours is shown in Fig.9.

(From http://www.gnssplanning.com)

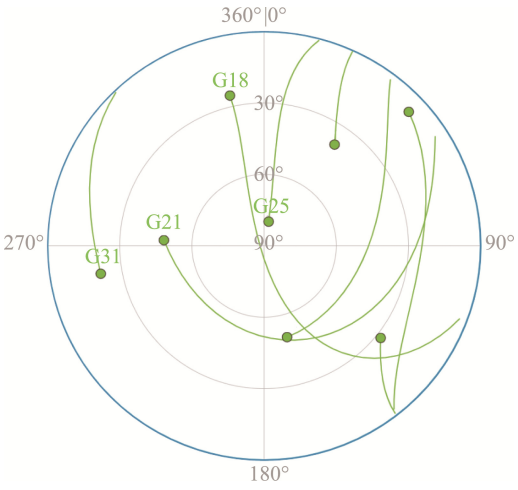

Fig.9 Satellites Sky Plot

5 Conclusion

Due to the complex space electromagnetic environment in signal transmission, the satellite signal quality is affected by ionospheric scintillation, which leads to the decrease of carrier-to-noise ratio of receiver and the increase of tracking error and positioning error. Especially in low latitudes and equatorial regions, severe ionospheric scintillation will lead to hours of navigation interruption. The software receiver improved in this paper realizes the detection of strong ionospheric scintillation in the equatorial regions and also realizes the successful acquisition, tracking, positioning and demodulation of satellite signals. The test results show that the horizontal positioning error can be controlled within 5 m, indicating that the software receiver is still reliable under the weak signal conditions caused by strong ionospheric scintillation. The improved software receiver can modify the scintillation detection threshold and detect ionospheric scintillation with different intensities, which provides important basis and useful guidance for analyzing ionospheric scintillation and space weather. This paper will be of significance for the future design of high-performance Beidou navigation receiver and also the territorial security of the South China Sea.

Acknowledgment

We would like to thank Professor Jade Morton and Professor Dennis M Akos in the University of Colorado at Boulder for providing the original measurement data of São José dos Campos, Brazil, and also thank their kind supports.

References

[1] Belakhovsky, V B. Jin, Y Q and Miloch, W J. (2021). Influence of Different Types of Ionospheric Disturbances on GPS Signals at Polar Latitudes. *Annales Geophysicae*, 39(4), pp.687-700.

[2] Yin, P. Li, Q Y. (2018). The Influence of Ionospheric E / F Layer Scintillation on GPS TEC Change Rate. *Journal of Civil Aviation University of China*, 36(5), pp.12-18.

[3] Jiao, Y. (2017). *Low-Latitude Ionospheric Scintillation*

Signal Simulation, Characterization, and Detection on GPS Signals. PhD. Colorado State University.

[4] Li, Q Y. and Yin, P. (2018). The Characteristic Study of Ionospheric Scintillations over China Based on GNSS Data. In: *Proceedings of the 9th China Satellite Navigation Academic Annual Conference*. Harbin: CSNAC, pp.190-195

[5] Cheng, J. Xu, J S. and Cai, L. (2018). A Comparison of Statistical Features of Ionospheric Scintillations and Cycle Slips in the Mid-South Region of China. *Chinese Journal of Geophysics*, 61(1), pp.18-29.

[6] Lan, W. and He, L. (2018). Analysis of Strong Ionospheric Scintillation Effects on Availability of Receiver. *Ship Electronic Engineering*. 38(10), pp. 204-206, 219.

[7] Mulugeta, S. and Kassa, T. (2022). Investigation of GPS Loss of Lock occurrence and Its characteristics over Ethiopia using Geodetic GPS receivers of the IGS network. *Advances in Space Research.* 69(2), pp.939-950.

[8] Huang, L F. Tian J P. and Zhao K. et al. (2019). Temporal and Spatial Characteristics of the Ionospheric Scintillation Event and the Influence on Communication in the Northern EIA Crest Region. *Chinese Journal of Space Science*, 39(2), pp.158-166.

[9] Zhu, X F. Chen, X Y. and Huang, H Q. et al. (2016). Analysis of GPS Ionospheric Scintillation Signal Amplitude Fading Characteristics at Low Latitude. *Journal of Southeast University*, 32(4), pp.484-488.

[10] Zhu, X F. Chen, X Y. and Chen, J F. (2016). Influence of Strong Ionospheric Scintillation on GPS Software Receiver. *Journal of Chinese Inertial Technology*, (4), pp.480-484.

[11] Zhu, X F. (2009). *Research on Key Techniques of High-Sensitivity GNSS Software Receivers*. PhD. Southeast University.

[12] Niu, F. (2012). *Performances of GPS Signal Observables Detrending Methods for Ionosphere Scintillation Studies*. PhD. Miami University

[13] Li, S. Yi, Q M. Chen, Q. and Shi M. et al. (2012). Weak Signal Acquisition Method for GPS Software Receiver. *Computer Application*, 32(3), pp.67-72.

Author Biographies

ZHU Xuefen received her Ph.D. degree from Southeast University in 2010. Now, she is an associate professor and master supervisor in Southeast University. Her main research interests include GNSS signal processing, GNSS/INS integration technology and detection on ionospheric scintillation.

E-mail: zhuxuefen@seu.edu.cn

LIN Mengying received the B.Sc. degree in electrical engineering and automation from Wuhan Institute of Technology, Wuhan, China, in 2017. She is currently a MD-PhD candidate in instrument science and technology in Southeast University, Nanjing, China. Her main research interests include interference detection on satellites' signals and GNSS signal processing technologies.

E-mail: 230198865@seu.edu.cn

LU Zhengpeng received the B.Sc. degree in measurement and control technology and instrument from Dalian Maritime University, China, in 2021. He is currently a M.Sc. candidate in the School of Instrument Science and Engineering, Southeast University, Nanjing, China. His main research interests include signal processing and interference detection on satellite signals.

E-mail: 220213669@seu.edu.cn

CHEN Xiyuan received his Ph.D. degree from Southeast University, Nanjing, China, in 1998. He is currently a Professor in the School of Instrument Science and Engineering, Southeast University. From October 2005 to September 2006, he was with the Department of Electronic Engineering, Politecnico di Torino, Italy, as a visiting scholar. He has authored or co-authored more than 200 papers and 60 granted patents. His main research interest includes fiber optic related application.

E-mail: chxiyuan@seu.edu.cn